Value of perfusion parameters and histogram analysis of triphasic computed tomography in pre-operative prediction of histological grade of hepatocellular carcinoma

Chun-Chun Shao[1], Fang Zhao[2], Yi-Fan Yu[3,4], Lin-Lin Zhu[5], Guo-Dong Pang[5]

[1]Department of Evidence-Based Medicine, The Second Hospital, Cheeloo College of Medicine, Shandong University, Jinan, Shandong 250033, China;
[2]Department of Radiology, Qilu Hospital, Cheeloo College of Medicine, Shandong University, Jinan, Shandong 250012, China;
[3]Healthcare Big Data Institute of Shandong University, Jinan, Shandong 250000, China;
[4]Department of Epidemiology and Health Statistics, School of Public Health, Shandong University, Jinan, Shandong 250000, China;
[5]Department of Radiology, The Second Hospital, Cheeloo College of Medicine, Shandong University, Jinan, Shandong 250033, China.

Abstract

Background: Pre-operative non-invasive histological evaluation of hepatocellular carcinoma (HCC) remains a challenge. Tumor perfusion is significantly associated with the development and aggressiveness of HCC. The purpose of the study was to evaluate the clinical value of quantitative liver perfusion parameters and corresponding histogram parameters derived from traditional triphasic enhanced computed tomography (CT) scans in predicting histological grade of HCC.

Methods: Totally, 52 patients with HCC were enrolled in this retrospective study and underwent triple-phase enhanced CT imaging. The blood perfusion parameters were derived from triple-phase CT scans. The relationship of liver perfusion parameters and corresponding histogram parameters with the histological grade of HCC was analyzed. Receiver operating characteristic (ROC) curve analysis was used to determine the optimal ability of the parameters to predict the tumor histological grade.

Results: The variance of arterial enhancement fraction (AEF) was significantly higher in HCCs without poorly differentiated components (NP-HCCs) than in HCCs with poorly differentiated components (P-HCCs). The difference in hepatic blood flow (HF) between total tumor and total liver flow ($\Delta HF = HF_{tumor} - HF_{liver}$) and relative flow ($rHF = \Delta HF/HF_{liver}$) were significantly higher in NP-HCCs than in P-HCCs. The difference in portal vein blood supply perfusion (PVP) between tumor and liver tissue (ΔPVP) and the ΔPVP/liver PVP ratio (rPVP) were significantly higher in patients with NP-HCCs than in patients with P-HCCs. The area under ROC (AUC) of ΔPVP and rPVP were both 0.697 with a high sensitivity of 84.2% and specificity of only 56.2%. The ΔHF and rHF had a higher specificity of 87.5% with an AUC of 0.681 and 0.673, respectively. The combination of rHF and rPVP showed the highest AUC of 0.732 with a sensitivity of 57.9% and specificity of 93.8%. The combined parameter of ΔHF and rPVP, rHF and rPVP had the highest positive predictive value of 0.903, and that of rPVP and ΔPVP had the highest negative predictive value of 0.781.

Conclusion: Liver perfusion parameters and corresponding histogram parameters (including ΔHF, rHF, ΔPVP, rPVP, and $AEF_{variance}$) in patients with HCC derived from traditional triphasic CT scans may be helpful to non-invasively and pre-operatively predict the degree of the differentiation of HCC.

Keywords: Hepatocellular carcinoma; Perfusion; Computed tomography; Histological grade; Histogram

Introduction

Hepatocellular carcinoma (HCC) is the fifth most common cancer and the third leading cause of cancer-related death worldwide.[1,2] Treatment methods include liver transplantation, surgical resection, radiofrequency ablation, transcatheter hepatic arterial chemoembolization, and targeted therapies.[3] Surgical resection is considered one of the most effective treatments for HCC. Even after undergoing curative resection, high recurrence rates in HCC (50%–60% at 3 years and 70%–100% at 5 years) have been documented in patients with evidence of the significantly negative outcome of HCC.[4] It has been shown that the histological grade of HCC could be used to predict long-term survival before liver transplantation or local treatment

Access this article online

Quick Response Code:

Website: www.cmj.org

DOI: 10.1097/CM9.0000000000001446

Chun-Chun Shao and Fang Zhao contributed equally to this work.

Correspondence to: Dr. Guo-Dong Pang, Department of Radiology, The Second Hospital, Cheeloo College of Medicine, Shandong University, Jinan, Shandong 250033, China
E-Mail: zhaofang27@126.com

Chinese Medical Journal 2021;134(10)

Received: 09-11-2020 **Edited by:** Xin Chen and Yuan-Yuan Ji

and is an independent predictor of post-operative recurrence.[5] Therefore, accurate prediction of histological grade is critical for clinical decision-making and prognosis. HCCs with poorly differentiated components (P-HCCs) have higher tumor recurrence rate, poorer prognosis, and lower survival rate, compared with moderately and well-differentiated HCC.[5,6] It has been shown that poor HCC histological grade is significantly correlated with unfavorable survival outcomes following liver transplantation, curative resection, and local therapies.[7,8] However, tumor histological evaluation is mostly feasible after the surgery and pathological exams. Therefore, pre-treatment non-invasive tumor histological evaluation is necessary for prognosis estimation. Studies have evaluated the correlation between blood supply and the histological grade for HCCs.[9,10] The development of HCC is associated with a progressively increasing arterial blood supply through angiogenesis.[11] Therefore, quantitative evaluation of the perfusion status of the tumor may be useful for assessing the aggressiveness and progression of HCC (from a high-grade dysplastic nodule to advanced HCC).

In recent years, several reports[12-15] on the histological classification of HCC have been published. Due to the heterogeneity or overlap of different histological classification methods, there may be some controversies.[16] Magnetic resonance imaging (MRI) has been used for the grading of HCC in the last 20 years, in which the most important and widely used is diffusion-weighted imaging (DWI). Several studies[13,14] showed that apparent diffusion coefficient (ADC) values from DWI can improve the value of MRI in the grading of HCC, but it does not reflect the changes in the tumor parenchyma. In addition, the accuracy of the ADC values from DWI in grading HCC is limited due to the discrepancy of *b* values. In recent years, amide proton transfer-weighted (APTw) imaging has been introduced to predict grading.[17] APTw MRI can indirectly detect cellular mobile proteins, without any exogenous contrast agent injection through the exchange between amide protons and bulk water protons. However, APTw may be affected by some tissue parameters. Recently, Wang *et al*[18] attempted to establish an ultrasound imaging-diagnostic system for histopathological grades of differentiation of HCC and provides encouraging data on Sonazoid contrast-enhanced ultrasound in the histological differential diagnosis of HCC, especially in early HCC. However, the diagnosis of the histological differentiation grade of HCC was based on the prerequisite of a definitive diagnosis of HCC.

In patients with liver diseases including hepatic tumors and liver parenchymal diseases, accurate assessment of the alternation of hepatic blood flow (HF), that is, changes in hepatic perfusion, can provide vital information for the appropriate management and prognosis prediction. Evaluation of these changes in hepatic perfusion can now be performed using perfusion computed tomography (PCT), dynamic contrast-enhanced MRI, or contrast-enhanced ultrasound.[17,18] CT perfusion is highly promising as a functional vascular imaging technique for tumor hemodynamics monitoring, which has been applied in the quantitative evaluation of perfusion status of HCC.[19-23] Liver PCT imaging can be used to obtain accurate blood flow values of HCC and normal liver parenchyma, and can quantitatively measure perfusion parameters. It has also helped to expand the role of CT from a purely anatomic imaging tool to a combined morphologic and functional technique. However, traditional CT perfusion of the liver is largely unfulfilled clinically due to concerns over high radiation dose or poor imaging quality (owing to the use of low-tube voltages to decrease the radiation dose). The dual maximum slope model, which was first proposed by Blomley *et al*,[24] is widely used. Using this model, standard triphasic CT, as a novel method, could estimate the blood supply status of the liver[25] and could acquire a series of perfusion parameters. We suppose those perfusion parameters, which were usually expressed as mean values, may be efficient in predicting the histological grade of HCC. Moreover, assessment of tumor heterogeneity with histogram analysis in acquired CT imaging data is superior for tumor grading, tumor recurrence, and predicting overall survival of brain glioma, cervical, and colorectal cancer.[9,10,26] To our knowledge, few studies have been reported to evaluate the clinical potential of CT perfusion quantitative measurement and histogram analysis in predicting the histological grade of HCC.

In the present study, we evaluated the significance of liver perfusion parameters and corresponding histogram parameters from traditional triphasic CT scans for the non-invasive prediction of the histological grade of HCC. The optimal parameters to identify different grades of HCC were also determined.

Methods

Ethical approval

This study was approved by the Institutional Review Board of the Second Hospital of Shandong University (KYLL-2015[LW]-0004) and was also conducted according to the principles of the *Declaration of Helsinki* and corresponding guidelines. All subjects gave written informed consent before inclusion in the study.

Patient selection

A total of 119 consecutive patients suspected of malignant hepatic lesions who underwent hepatic resection between January 2017 and May 2019 were enrolled. All enrolled patients received tri-phase enhanced CT scan ($n = 105$), and then underwent partial hepatectomy ($n = 81$) or anatomic hemihepatectomy ($n = 24$) within 30 days. Fifty-three patients were excluded for the following reasons: the arterially enhancing portion of the tumor was too small to characterize (≤ 5 mm) ($n = 10$); previous anti-tumor treatments ($n = 16$); interval >1 month between triphasic CT scans and surgery ($n = 16$); patients with any kind of portal thrombosis (either in the main portal vein or in the segmental vessels) ($n = 7$), or more than three concurrent lesions ($n = 4$). Finally, 52 patients with pathologically confirmed HCCs were included for analysis. The study flowchart is shown in Figure 1.

Pathological evaluation of HCC specimens was performed by two experienced pathologists blinded to the radiologic findings. The degree of tumor cell differentiation was

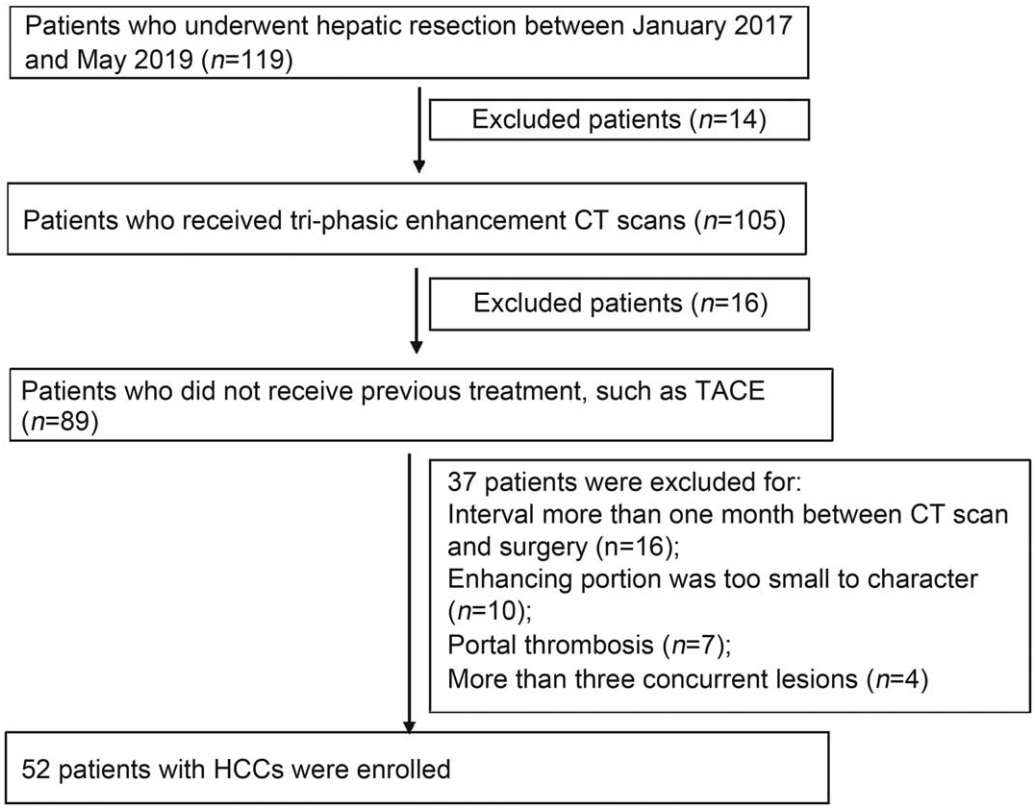

Figure 1: Flow diagram of patient inclusion and exclusion. CT: Computed tomography; TACE: transcatheter arterial chemoembolization; HCC: hepatocellular carcinoma.

classified by tumor grade as grades I–IV according to Edmondson-Steiner grading.[27]

Multi-detector CT protocols

All patients underwent non-contrast and triphasic contrast-enhanced CT scans on a Discovery 750HD CT scanner (GE Healthcare, Waukesha, WI, USA). Patients were fasted for 4 h and drank 500 to 800 mL warm water orally 5 to 10 min before the scanning. For each patient, 100 mL of iodinated contrast (Omnipaque 370 mg iodine/mL, GE) followed by a 30 mL saline chaser was injected intravenously at a rate of 3.0 to 4.0 mL/s. After an unenhanced CT scan was obtained, arterial phase (30–35 s), portal venous phase (60–70 s), and delayed phase (180 s) were performed after contrast injection. The scanning parameters were as follows: 128 × 0.625 mm collimation, 80 to 120 kV tube voltage, 200 mA effective tube current-time product, and 1.375 pitch, 0.5 s/rotation gantry rotation speed, 5 mm slice thickness. The volumetric CT dose index (CTDIvol) was 24.8 ± 3.2 mGy. Patients were instructed to hold their breath during the scanning.

Perfusion parameters measurements

Tumor regions of interest (ROIs) were drawn around the entire section of the tumor on three or four representative slices to eliminate bias. Tumor-free ROIs were drawn in the same lobe as the tumor and were of the same size as the tumor, excluding large intrahepatic vessels. CT hemodynamic kinetics software (CT Kinetics, GE Healthcare) was used to calculate hepatic arterial supply perfusion (HAP), portal vein blood supply perfusion (PVP), and arterial enhancement fraction (AEF) based on the model-free maximum method. The HAP, PVP, and AEF were measured in the tumor and normal liver tissue (tumor-free area) in each patient by two radiologists. AEF was defined as the ratio of the absolute increment of attenuation during the arterial phase to the absolute increment of attenuation during the portal venous phase. The perfusion parameters were calculated, including total HF_{tumor} ($HF_{tumor} = HAP_{tumor} + PVP_{tumor}$), total HF_{liver} ($HF_{liver} = HAP_{liver} + PVP_{liver}$), difference in flow between tumor and liver ($\Delta HF = HF_{tumor} - HF_{liver}$), relative flow ($rHF = \Delta HF/HF_{liver}$), difference in HAP ($\Delta HAP = HAP_{tumor} - HAP_{liver}$), relative HAP ($rHAP = \Delta HAP/HAP_{liver}$), difference in PVP ($\Delta PVP = PVP_{tumor} - PVP_{liver}$), relative PVP ($rPVP = \Delta PVP/PVP_{liver}$), difference in AEF ($\Delta AEF = AEF_{tumor} - AEF_{liver}$), and relative AEF ($rAEF = \Delta AEF/AEF_{liver}$). From these voxel-by-voxel HAP, PVP, and AEF values, a histogram for each lesion was generated using statistical analysis software (JMP Pro, version 9.0, SAS Institute Inc., Cary, NC, USA), including median, mean, standard deviation (SD), 10th to 90th percentile, variance, skewness, and kurtosis.[28-30]

Estimation of sample size and outcome evaluation

To estimate the sample size required to demonstrate the difference between different HCC grading phases, a prior sample size calculation was conducted by using G*Power

3.1.9.4 software (Program written by Franz Faul, University Kiel, Germany). Under the condition of alpha at 0.05, power at 0.8, and allocation ratio P-HCC/NP-HCC at 1:3, a total of 18 lesions (14 NP-HCC lesions and four P-HCC lesions) would be sufficient to achieve an effect size of 1.6, corresponding to a difference of about 10 unit of attenuation values while a total of 52 lesions (36 NP-HCC lesions and 16 P-HCC lesions) would achieve an effect size of 1.0, corresponding to a difference of about 6 unit of attenuation values.

Clinicopathological information of all patients was collected from the medical records, including sex, age, tumor size, etiology, and Child-Pugh stage. All patients were divided into two groups: HCCs without poorly differentiated components (NP-HCCs) (Edmondson grade I or II) and P-HCCs (Edmondson III or IV). The association between histopathological grade and perfusion parameters and histogram values was evaluated.

Statistical analyses

All statistical analyses were performed in R version 3.6.1 (the R core team, the Statistics Department of the University of Auckland, New Zealand). Inter-observer agreement between the two radiologists was assessed by weighted *k* statistics. Degrees of agreement were categorized as follows: 0.00 to 0.20, poor agreement; 0.20 to 0.39, fair agreement; 0.40 to 0.59, moderate agreement; 0.60 to 0.79 substantial agreement, and 0.80 to 1.00, excellent agreement. If there was disagreement between observers, an agreement was achieved by discussion. Kolmogorov-Smirnov test was performed to analyze the normality of data. Data of normal distribution were expressed as mean ± SD and analyzed with the independent samples *t*-test. Data of non-normal distribution were expressed as median (P25, P75) and analyzed with a non-parametric rank-sum test (Mann-Whitney *U* test). Fisher discrimination criterion, also known as the canonical criterion, applied to two categories (P-HCCs and NP-HCCs) of this study. Receiver operating characteristic (ROC) curve analysis was performed to determine the optimal cutoff value of each parameter for predicting the histopathological grade of HCC, and the corresponding sensitivity and specificity. A P value < 0.05 was considered to be significant.

Results

Clinical and pathological characteristics of the patients

Table 1 showed the baseline clinical characteristics of the 52 patients with HCCs in this study, including 36 males and 16 females, with a mean age of 52.8 years (range, 30–85 years). According to their liver function by Child-Pugh classification, there were 38 (77%) patients in the Child-Pugh class A group and 14 (23%) patients in the Child-Pugh class B/C group. Hepatitis virus markers were positive in 45 (87%) of 52 patients, including 30 (58%) cases with positive hepatitis B surface antigen and 15 (29%) cases with positive hepatitis C. Only seven (13%) patients had a significant alcohol history. The mean diameter of the tumor was 11.4 ± 7.8 mm (range, 4–67 mm). The number of cases with poor, moderate, and well-differentiated HCC was 16, 25, and 11, respectively. There were no significant differences in the following clinical characteristics between the two groups: age, history of hepatitis virus, sex, liver function, and etiology of the liver disease (all $P > 0.05$).

Table 1: Baseline characteristics of patients with P-HCCs or NP-HCCs.

Clinical features	P-HCCs (*n*=16)	NP-HCCs (*n*=36)	Statistics	*P*
Age (years)	53.0 ± 12.8	50.7 ± 13.5	$t = 1.349$	0.641
Sex			$\chi^2 = 0.000$	1.000
Male	11 (69)	25 (69)		
Female	5 (31)	11 (31)		
Etiology			$\chi^2 = 0.853$	0.653
Hepatitis B	8 (50)	22 (61)		
Hepatitis C	6 (38)	9 (25)		
Alcoholism	2 (12)	5 (14)		
Child-Pugh classification			$\chi^2 = 0.652$	0.419
A	10 (78)	28 (68)		
B/C	6 (22)	8 (32)		
Tumor size (mm)	21.3 ± 9.4	13.1 ± 7.6	$t = 1.537$	0.144
Hepatic background			$\chi^2 = 4.115 \times 10^{-31}$	0.978
Fibrosis	3 (19)	6 (17)		
Cirrhosis	13 (81)	30 (83)		
AFP level			$\chi^2 = 1.428$	0.490
≤10 ng/mL	0	3 (8)		
10–400 ng/mL	7 (44)	15 (42)		
≥400 ng/mL	9 (56)	18 (50)		

Data were shown as mean ± standard deviation, or *n* (%). AFP: Alpha-fetoprotein; HCCs: Hepatocellular carcinomas; NP-HCCs: HCCs without poorly differentiated components; P-HCCs: HCCs with poorly differentiated components.

Correlation of perfusion parameters and corresponding histogram parameters with the histopathological grade of HCC

The data of perfusion parameters and histogram parameters were of non-normal distribution. Therefore, the Mann-Whitney *U* test was performed for data analysis. The perfusion parameters of P-HCC and NP-HCC were presented in Table 2. The typical CT images with perfusion parameters and corresponding histogram parameters were shown in Figure 2. The difference in flow between total tumor and total liver flow ($\Delta HF = HF_{tumor} - HF_{liver}$) and

Table 2: Liver perfusion parameters in patients with P-HCCs or NP-HCCs.

	P-HCCs ($n = 16$)			NP-HCCs ($n = 36$)				
Parameters	**Median**	**P25**	**P75**	**Median**	**P25**	**P75**	***W*-value**	***P***
HF	0.250	0.212	0.294	0.260	0.224	0.294	277	0.619
ΔHF	−0.101	−0.151	−0.070	−0.038	−0.110	0.012	194	0.037*
rHF	−0.305	−0.397	−0.186	−0.124	−0.328	0.034	199	0.046*
ΔHAP	−0.047	−0.067	−0.015	−0.052	−0.084	−0.008	339	0.517
rHAP	−0.601	−3.261	0.520	−0.678	−2.547	0.285	291	0.815
ΔPVP	−0.152	−0.161	−0.118	−0.096	−0.135	−0.047	184	0.022*
rPVP	−0.387	−0.401	−0.330	−0.284	−0.359	−0.165	184	0.022*
ΔAEF	0.044	0.030	0.074	0.049	0.026	0.078	281	0.673
rAEF	0.089	0.059	0.158	0.010	0.051	0.167	281	0.673

HF, ΔHF, ΔHAP, and ΔPVP values are expressed as mL/100 mL/min. rHF, rHAP, rPVP, rAEF, and ΔAEF values are expressed as fractions (no units). *Statistically significant difference between the two groups ($P < 0.05$). ΔAEF: Difference of arterial enhancement fraction ($AEF_{tumor} - AEF_{liver}$); ΔHAP: Difference of hepatic arterial perfusion ($HAP_{tumor} - HAP_{liver}$); ΔHF: Difference in blow between tumor and liver ($HF_{tumor} - HF_{liver}$); ΔPVP: Difference of portal vein perfusion ($PVP_{tumor} - PVP_{liver}$); HCCs: Hepatocellular carcinomas; HF: Hepatic blood flow; rAEF: Relative arterial enhancement fraction ($\Delta AEF/AEF_{liver}$); rHAP: Relative hepatic arterial perfusion ($\Delta HAP/HAP_{liver}$); rHF: Relative total tumor flow ($\Delta HF/HF_{liver}$); rPVP: Relative portal vein perfusion ($\Delta PVP/PVP_{liver}$).

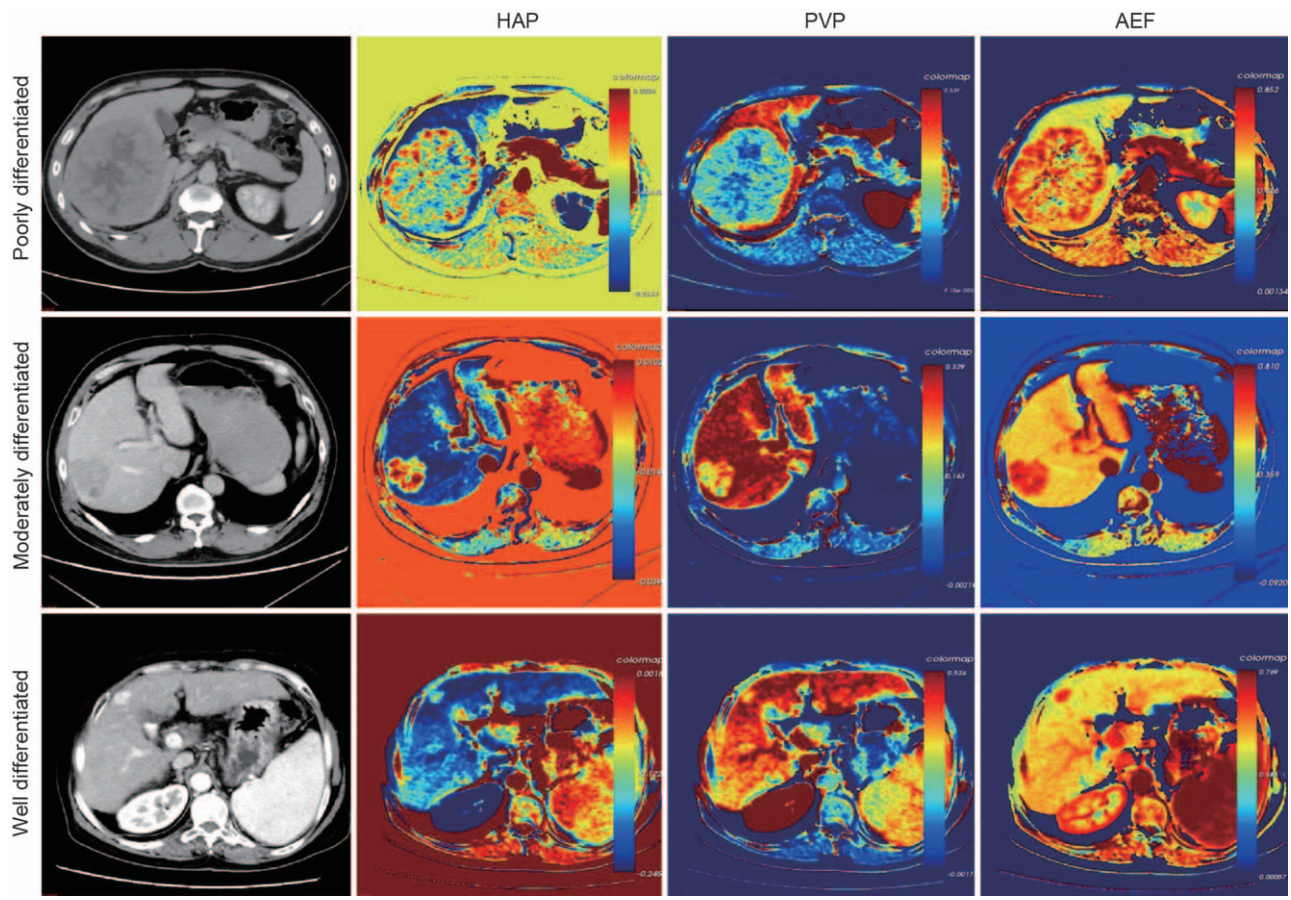

Figure 2: Traditional enhancement image and pharmacokinetic images of the P-HCCs and NP-HCCs. For the patients with different histological grades, all AEF and HAP images showed heterogeneous (P-HCC and M-HCC) and homogeneous (W-HCC) high perfusion in the lesions; all PVP images showed heterogeneous (P-HCC and M-HCC) and homogeneous (W-HCC) low perfusion in the lesions. AEF: Arterial enhancement fraction; HAP: Hepatic arterial supply perfusion; HCC: Hepatocellular carcinoma; NP-HCC: Non-poorly differentiated HCC; P-HCC: Poorly differentiated HCC; PVP: Portal venous supply perfusion.

Table 3: Histogram parameters of patients with P-HCCs or NP-HCCs.

	P-HCCs ($n = 16$)			NP-HCCs ($n = 36$)				
Parameters	Median	P25	P75	Median	P25	P75	*W*-value	*P*
HAP_Median	0.001	−0.018	0.012	0.019	−0.010	0.031	236	0.203
HAP_Mean	0.001	−0.017	0.012	0.020	−0.013	0.031	240	0.232
HAP_Std	0.011	0.008	0.014	0.011	0.008	0.015	298	0.918
HAP_Variance	0.0001	5.888	0.0002	0.0001	5.662	0.0002	307	0.963
HAP_Skewness	0.190	−0.110	0.381	0.004	−0.180	0.253	347	0.425
HAP_Kurtosis	2.961	2.782	3.359	3.014	2.788	4.089	279	0.646
HAP_10	−0.006	−0.033	0.003	0.004	−0.031	0.021	241	0.239
HAP_25	−0.003	−0.027	0.007	0.012	−0.021	0.026	236	0.203
HAP_50	0.0004	−0.018	0.012	0.020	−0.011	0.031	237	0.210
HAP_75	0.006	−0.007	0.017	0.024	−0.004	0.038	246	0.279
HAP_90	0.012	0.003	0.020	0.030	0.003	0.044	248	0.296
PVP_Median	0.257	0.217	0.292	0.261	0.223	0.306	298	0.918
PVP_Mean	0.259	0.216	0.296	0.258	0.216	0.306	298	0.918
PVP_Std	0.058	0.050	0.076	0.054	0.042	0.061	380	0.154
PVP_Variance	0.003	0.002	0.006	0.003	0.002	0.004	381	0.149
PVP_Skewness	0.154	−0.066	0.313	0.043	−0.401	0.319	347	0.425
PVP_Kurtosis	3.373	2.824	3.956	3.143	2.762	4.289	289	0.786
PVP_10	0.181	0.124	0.231	0.191	0.153	0.244	272	0.554
PVP_25	0.221	0.168	0.257	0.225	0.182	0.274	280	0.659
PVP_50	0.258	0.217	0.292	0.261	0.222	0.306	300	0.948
PVP_75	0.305	0.257	0.329	0.293	0.258	0.346	317	0.815
PVP_90	0.338	0.296	0.379	0.324	0.289	0.387	320	0.771
AEF_Median	0.550	0.533	0.594	0.573	0.540	0.621	245.5	0.271
AEF_Mean	0.554	0.532	0.596	0.577	0.543	0.624	246	0.279
AEF_Std	0.068	0.048	0.083	0.057	0.043	0.074	352	0.372
AEF_Variance	0.005	0.002	0.007	0.003	0.002	0.006	336	0.047*
AEF_Skewness	0.108	−0.458	1.079	0.213	−0.192	0.835	270	0.530
AEF_Kurtosis	7.619	4.382	17.129	3.488	3.011	10.459	403	0.062
AEF_10	0.480	0.460	0.524	0.521	0.470	0.556	222	0.123
AEF_25	0.512	0.499	0.565	0.540	0.502	0.582	240	0.232
AEF_50	0.550	0.532	0.594	0.572	0.542	0.622	246	0.279
AEF_75	0.602	0.558	0.629	0.610	0.569	0.659	258	0.393
AEF_90	0.640	0.583	0.690	0.657	0.595	0.703	272	0.554

*Statistically significant difference between the two groups ($P < 0.05$). AEF: Arterial enhancement fraction (%); HAP: Hepatic artery perfusion (mL/100 mL/min); HCCs: Hepatocellular carcinomas; PVP: Portal vein perfusion (mL/100 mL/min).

relative flow (rHF = $\Delta HF/HF_{liver}$) were significantly higher in NP-HCCs than in P-HCCs ($P = 0.037$ and $P = 0.046$, respectively). The difference in PVP between tumor and liver tissue (ΔPVP) and the ΔPVP/liver PVP ratio (rPVP) were significantly higher in patients with NP-HCCs than in patients with P-HCCs ($P = 0.022$ and $P = 0.022$, respectively). There were no significant differences in the other perfusion parameters tested between the two groups.

The histogram parameters for each group are shown in Table 3. The variance of AEF was higher in patients with NP-HCCs than with P-HCCs ($P = 0.047$). For the other histogram parameters, there were no statistically significant differences between P-HCCs and NP-HCCs.

Predictive ability of perfusion parameters and corresponding histogram parameters for the histopathological grade of HCC

ROC analysis was used to assess the discriminant ability of the statistically significant variables in all liver perfusion parameters and histogram parameters to differentiate between the P-HCC group and NP-HCC group. As shown in Figure 3 and Table 4, the AUC for ΔHF was 0.681, and the sensitivity and specificity were 57.5% and 87.5%, respectively ($P < 0.05$) with a cutoff value of −0.056. The positive predictive value (PPV) and negative predictive value (NPV) were 0.822 and 0.675, respectively. The AUC for rHF was 0.673. The sensitivity, specificity, and cutoff value of rHF were 52.6%, 87.5%, and −0.142, respectively. The PPV was 0.808, and the NPV was 0.649. For ΔPVP and rPVP, both of the AUC were 0.697, with sensitivity and specificity of 84.2% and 56.2%, respectively. The cutoff value of ΔPVP was −0.147 and that of rPVP was −0.379. The PPV and NPV were 0.658 and 0.781, respectively, which were the same between rPVP and ΔPVP. The parameter of rPVP and ΔPVP had the highest NPV value of 0.781. The AUC of the variance of AEF was 0.579, and the sensitivity and specificity were 60.5% and 62.5%, respectively, with a cutoff value of 0.004, and the PPV and NPV were 0.647 and 0.663, respectively.

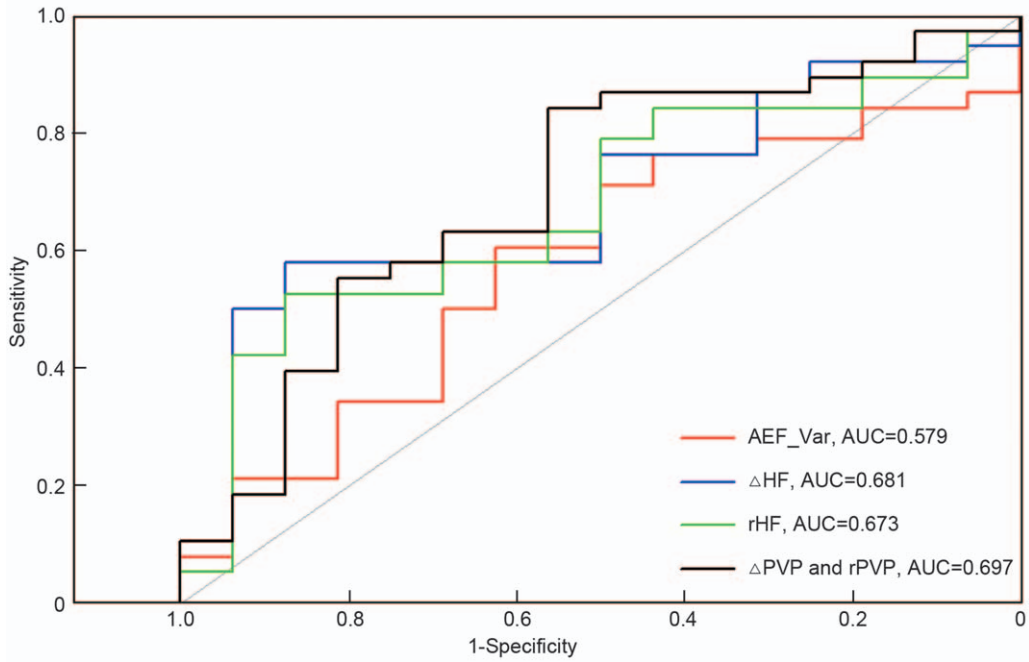

Figure 3: The ROC analysis of ΔHF, rHF, ΔPVP, rPVP, and $AEF_{variance}$ for P-HCCs and NP-HCCs. ΔHF: Difference in blow between tumor and liver ($HF_{tumor} - HF_{liver}$); ΔPVP: Difference of portal vein perfusion ($PVP_{tumor} - PVP_{liver}$); $AEF_{variance}$: The variance value of arterial enhancement fraction; AUC: Area under the curve; HCCs: Hepatocellular carcinomas; HF: Hepatic blood flow; rHF: Relative total tumor flow ($\Delta HF/HF_{liver}$); ROC: Receiver operating characteristic; rPVP: Relative portal vein perfusion ($\Delta PVP/PVP_{liver}$).

Table 4: ROC analysis of ΔHF, rHF, ΔPVP, rPVP, and $AEF_{variance}$ in the differentiation of pathological grades of HCCs.

Variables	AUC	Sensitivity, %	Specificity, %	Cutoff value	NPV	PPV
ΔHF	0.681	57.9	87.5	−0.056	0.675	0.822
rHF	0.673	52.6	87.5	−0.142	0.649	0.808
ΔPVP	0.697	84.2	56.2	−0.147	0.781	0.658
rPVP	0.697	84.2	56.2	−0.379	0.781	0.658
$AEF_{variance}$	0.579	60.5	62.5	0.004	0.663	0.647

ΔHF and ΔPVP values are expressed as mL/100 mL/min. rHF and rPVP values are expressed as fractions (no units). ΔHAP: Difference of hepatic arterial perfusion ($HAP_{tumor} - HAP_{liver}$); ΔHF: Difference in blow between tumor and liver ($HF_{tumor} - HF_{liver}$); ΔPVP: Difference of portal vein perfusion ($PVP_{tumor} - PVP_{liver}$); $AEF_{variance}$: The variance value of arterial enhancement fraction; AUC: Area under the curve; HCCs: Hepatocellular carcinomas; HF: Total tumor flow; NPV: Negative predictive value; PPV: Positive predictive value; rHAP: Relative hepatic arterial perfusion ($\Delta HAP/HAP_{liver}$); rHF: Relative total tumor flow ($\Delta HF/HF_{liver}$); ROC: Receiver operating characteristic; rPVP: Relative portal vein perfusion ($\Delta PVP/PVP_{liver}$).

The parameters with the highest sensitivity and specificity were combined in pairs to predict the histological grades of HCCs. As shown in Table 5, the combined parameter of rHF and rPVP, ΔHF and ΔPVP yielded the highest AUC of 0.732 with integrated discrimination improvement and net reclassification improvement of 0.599 and 0.349, respectively. For the combined parameter of rHF and rPVP, the sensitivity and specificity were 57.9% and 93.8%, respectively. For the combined parameter of ΔHF and ΔPVP, the sensitivity and specificity were 63.2% and 87.5%, respectively. The combined parameter of rHF and rPVP also showed the highest specificity [Figure 4]. The combined parameter of ΔHF and rPVP, rHF and rPVP had the highest PPV value of 0.903, and the combined parameter of ΔPVP and rHF, and ΔPVP and ΔHF had the NPV value of 0.704.

Inter-observer agreement

To evaluate inter-observer agreement in terms of liver perfusion parameters and HCC histogram parameters analysis, the quadratic weighted *k* statistics were performed. The quantitative analyses of liver perfusion parameters and corresponding histogram parameters of HCC exhibited excellent inter-observer agreement ($k = 0.85$). Therefore, the quantitative analysis of perfusion and histogram parameters were used for further analysis.

Discussion

PCT of the liver is regarded as a valuable tool that can provide liver perfusion parameters, which reflect the hemodynamic changes and expand the role of CT as a morphologic-functional technique. However, the application of PCT in clinical practice is limited owing to large radiation exposure or poor imaging quality. Presently, the dual maximum slope model, which was first described by Blomley *et al*,[24] is widely used. Based on this model, HAP and PVP can be calculated by dividing the peak gradient of the liver time-attenuation curve before peak splenic

Table 5: ROC analysis of the combined parameters in the differentiation of pathological grades of HCCs.

Variables	AUC	Sensitivity, %	Specificity, %	Cutoff value	NPV	PPV
ΔHF + ΔPVP	0.732	63.2	87.5	−0.169	0.704	0.835
rHF + ΔPVP	0.709	63.2	87.5	−0.220	0.704	0.835
ΔHF + rPVP	0.715	57.9	93.8	0.000	0.690	0.903
rHF + rPVP	0.732	57.9	93.8	−0.201	0.690	0.903

ΔHF and ΔPVP values are expressed as mL/100 mL/min. rHF and rPVP values are expressed as fractions (no units). ΔHAP: Difference of hepatic arterial perfusion ($HAP_{tumor} - HAP_{liver}$); ΔHF: Difference in blow between tumor and liver ($HF_{tumor} - HF_{liver}$); ΔPVP: Difference of portal vein perfusion ($PVP_{tumor} - PVP_{liver}$); $AEF_{variance}$: The variance value of arterial enhancement fraction; AUC: Area under the curve; HCCs: Hepatocellular carcinomas; HF: Total tumor flow; NPV: Negative predictive value; PPV: Positive predictive value; rHAP: Relative hepatic arterial perfusion ($\Delta HAP/HAP_{liver}$); rHF: Relative total tumor flow ($\Delta HF/HF_{liver}$); ROC: Receiver operating characteristic; rPVP: Relative portal vein perfusion ($\Delta PVP/PVP_{liver}$).

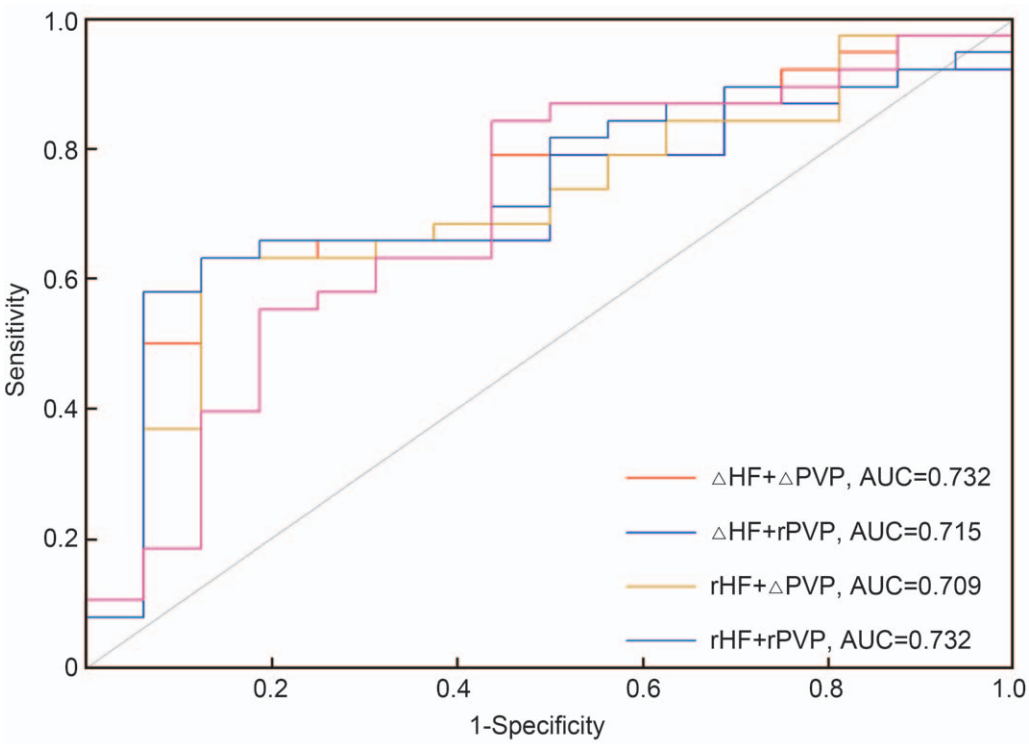

Figure 4: The ROC analysis of the combined parameters in the differentiation of pathological grades of HCCs including the parameters of rHF + rPVP, rHF + ΔPVP, rPVP + ΔHF, ΔHF + ΔPVP. ΔHF: Difference in blow between tumor and liver ($HF_{tumor} - HF_{liver}$); ΔPVP: Difference of portal vein perfusion ($PVP_{tumor} - PVP_{liver}$); $AEF_{variance}$: The variance value of arterial enhancement fraction; AUC: Area under the curve; HCCs: Hepatocellular carcinomas; HF: Hepatic blood flow; rHF: Relative total tumor flow ($\Delta HF/HF_{liver}$); ROC: Receiver operating characteristic; rPVP: Relative portal vein perfusion ($\Delta PVP/PVP_{liver}$).

enhancement by the peak aortic enhancement. Lee *et al*[31] reported that liver perfusion parameters could be obtained from traditional dynamic CT scans using the dual maximum slope model and that no significant differences were observed between perfusion parameters derived from traditional dynamic CT scans and from real PCT in liver parenchyma and HCCs. Recently, a traditional triphasic scan with a simplified model of tumor blood supply has been developed and validated. The linear combination of the enhancement curves of the aorta and portal vein could be used to calculate the hepatic artery and portal vein blood supply coefficients of the tumor.[28] The pre-treatment non-invasive detection and assessment of histological differentiation remains a challenge.[13,14,32] For the majority of patients, histological evaluation mainly depends on specimens from surgery or biopsy. PCT is a highly promising vascular imaging technique, which has been applied in HCC. In the present study, we developed a simplified model of tumor blood supply that can be applied to standard triphasic CT scans. Analysis using CT hemodynamic kinetics software was performed to calculate various parameters obtained from the standard triphasic CT. Thus, the radiation dose by volume (CTDIvol) of triphasic CT scan was considerably lower than that of traditional perfusion imaging. On the other hand, this model based on a routine triphasic scan could calculate various parameters, which provide functional information about the microcirculation of normal parenchyma and focal liver lesions. By contrast, a triphasic enhancement CT scan can only provide morphologic imaging, which may not fully assess the tumor.

The current study showed that the quantitative perfusion parameters in patients with HCC changed significantly

among different histological grades. This study demonstrated the values of ΔHF, rHF, ΔPVP, rPVP, and $AEF_{variance}$ for predicting HCC histological grade and for discriminating P-HCCs from NP-HCCs. All the parameters mentioned above were significantly higher for P-HCCs than for NP-HCCs. The parameter of ΔPVP and rPVP both showed a higher AUC of 0.697 than other parameters, which were considered effective for estimating the HCC histological grade. In addition, we evaluated the role of combined parameters in the prediction of histological grades. The combined parameter of rHF and rPVP, and ΔHF and ΔPVP showed the highest AUC of 0.732, which showed the best predictive power for discriminating P-HCCs from NP-HCCs. However, the AUC value of the combined parameters was still relatively low. This may be because of the small sample size or some measurement error. Studies have shown that perfusion parameters derived from triphasic CT scans can provide functional information regarding the microcirculation of the normal parenchyma and focal liver lesions, and can assess the efficacy of various anti-cancer treatments.[33,34] In addition, in the study by Hsu *et al*,[35] perfusion parameters were shown to correlate well with tumor survival and treatment response in patients with HCC who received anti-angiogenic drugs. Therefore, we believe that this modality can also provide important information for the management of patients with chronic liver disease and liver malignancies while reducing the radiation dose, rather than just providing morphologic information. Next, we will continue further research to improve its predictive value by increasing the sample size and reducing the error.

The present study involved the retrospective analysis of the efficacy of PCT derived from traditional triphasic CT scans in differentiating the histological grade in patients with HCC. Our results indicate that ΔHF and rHF were significantly higher in NP-HCCs than in P-HCCs. This may be caused by the reason that, patients with NP-HCCs (well and moderately) frequently have an increased arterial blood supply, whereas those with p-HCCs have a decreased arterial blood supply.[36] The portal blood supply also decreases with the advancement of the tumor, and eventually, the tumor is fed mainly by the arterial flow.[25] So, in theory, the values of HF_{tumor} ($HF_{tumor} = HAP_{tumor} + PVP_{tumor}$) of NP-HCCs are higher than the values of P-HCCs. It is reported that[30] the values of HF_{tumor} may be influenced by the injection protocol and scanning equipment. This could limit the utility of HF_{tumor} as parameters for assessing the histological grade. However, in our study, a major advantage of ΔHF and rHF is that it is a self-normalizing quantity that has the potential to overcome all of these effects. Hence, the standardization of parameters such as ΔHF and rHF would be expected to reduce the differences caused by different equipment or PCT protocol or individual differences of liver blood circulation of different Child-Pugh classification.[37] In this study, the difference in PVP between tumor and liver tissue (ΔPVP) and the ΔPVP/liver PVP ratio (rPVP) were also significantly higher in patients with NP-HCCs than in patients with P-HCCs. The reason is the same as the data above (ΔHF and rHF). These findings could provide a basis for a more accurate clinical diagnosis of the histological grade, thus improving clinical decision-making in patients with HCCs. Tumor PCT typically is reported as a mean perfusion value. However, mean values do not account for the heterogeneity of tumors and thus may not be optimal for tumor evaluation. Description of heterogeneity of CT tumor perfusion with histogram analysis has shown to be superior to median values for tumor grading.[9,10] The results of our study showed that the variance of AEF based on the entire tumor volume could be used to differentiate P-HCCs from NP-HCCs. These values of AEF were significantly higher in patients with NP-HCCs than with P-HCCs. The results may reflect the more prominent arterial supply of NP-HCCs compared with P-HCCs.

For the discriminant ability of the statistically significant variables in all liver perfusion parameters and histogram parameters to differentiate between the two groups, the AUC of ΔPVP and rPVP was slightly higher than those of ΔHF, rHF, and $AEF_{variance}$. This result reflected that the differentiation ability of ΔPVP and rPVP was superior to the ability of the other single parameter. For ΔPVP and rPVP, they both had a sensitivity of 84.2% and specificity of only 56.2%, and the ΔHF and rHF both had a higher specificity of 87.5% in the differentiation of pathological grades. By contrast, the combined parameter of rHF and rPVP, and ΔHF and ΔPVP yielded the highest AUC of 0.732. It indicated that the prediction ability of the combined parameters was superior to all the single parameters. The combined parameter of rHF and rPVP showed the highest specificity of 93.8%. The combined parameter of ΔHF and rPVP, rHF and rPVP had the highest PPV value of 0.903, and the parameter of rPVP and ΔPVP had the highest NPV value of 0.781. The reason may be that portal venous blood flow and total blood flow change greatly as the tumor histological grade increases.

Several limitations of this study should be mentioned. First, the study sample was relatively small. Further investigation that includes a larger population is warranted to strengthen the statistical power. Second, this study was performed retrospectively in our single department of radiology. There might have been a selection bias. Third, our software only permitted the application of ROIs drawn in a single plane. It was not possible to use volumes of interest for the analysis of liver perfusion parameters, which could potentially lead to false-negative results.[38]

To conclude that liver perfusion parameters and corresponding histogram parameters of the tumor area derived from triphasic CT scans provide a quantitative, non-invasive method for predicting the histopathological grade of HCC.

Conflicts of interest

None.

References

1. Forner A, Reig M, Bruix J. Hepatocellular carcinoma. Lancet 2018;391:1301–1314. doi: 10.1016/S0140-6736(18)30010-2.
2. Chen W, Zheng R, Baade PD, Zhang S, Zeng H, Bray F, *et al*. Cancer statistics in China, 2015. CA Cancer J Clin 2016;66:115–132. doi: 10.3322/caac.21338.

3. Komorizono Y, Oketani M, Sako K, Yamasaki N, Shibatou T, Maeda M, *et al*. Risk factors for local recurrence of small hepatocellular carcinoma tumors after a single session, single application of percutaneous radiofrequency ablation. Cancer 2003;97:1253–1262. doi: 10.1002/cncr.11168.
4. Verslype C, Rosmorduc O, Rougier P. ESMO Guidelines Working Group. Hepatocellular carcinoma: ESMO-ESDO clinical practice guidelines for diagnosis, treatment and follow-up. Ann Oncol 2012;23 (Suppl 7):vii41–vii48. doi: 10.1093/annonc/mds225.
5. Kim SH, Lee WJ, Lim HK, Park CK. SPIO-enhanced MRI findings of well-differentiated hepatocellular carcinomas: correlation with MDCT findings. Korean J Radiol 2009;10:112–120. doi: 10.3348/kjr.2009.10.2.112.
6. Jonas S, Bechstein WO, Steinmuller T, Herrmann M, Radke C, Berg T, *et al*. Vascular invasion and histopathologic grading determine outcome after liver transplantation for hepatocellular carcinoma in cirrhosis. Hepatology 2001;33:1080–1086. doi: 10.1053/jhep.2001.23561.
7. Oishi K, Itamoto T, Amano H, Fukuda S, Ohdan H, Tashiro H, *et al*. Clinicopathologic features of poorly differentiated hepatocellular carcinoma. J Surg Oncol 2007;95:311–316. doi: 10.1002/jso.20661.
8. Kim SH, Lim HK, Choi D, Lee WJ, Kim SH, Kim MJ, *et al*. Percutaneous radiofrequency ablation of hepatocellular carcinoma: effect of histologic grade on therapeutic results. AJR Am J Roentgenol 2006;186:S327–S333. doi: 10.2214/AJR.05.0350.
9. Mayr NA, Yuh WT, Arnholt JC, Ehrhardt JC, Sorosky JI, Magnotta VA, *et al*. Pixel analysis of MR perfusion imaging in predicting radiation therapy outcome in cervical cancer. J Magn Reson Imaging 2000;12:1027–1033. doi: 10.1002/1522-2586(200012)12:6<1027::aid-jmri31>3.0.co;2-5.
10. Ng F, Ganeshan B, Kozarski R, Miles KA, Goh V. Assessment of primary colorectal cancer heterogeneity by using whole-tumor texture analysis: contrast-enhanced CT texture as a biomarker of 5-year survival. Radiology 2013;266:177–184. doi: 10.1148/radiol.12120254.
11. Park YN, Yang CP, Fernandez GJ, Cubukcu O, Thung SN, Theise ND. Neoangiogenesis and sinusoidal "capillarization" in dysplastic nodules of the liver. Am J Surg Pathol 1998;22:656–662. doi: 10.1097/00000478-199806000-00002.
12. Kondo F. Histological features of early hepatocellular carcinomas and their developmental process: for daily practical clinical application. Hepatol Int 2008;3:283–293. doi: 10.1007/s12072-008-9107-9.
13. Nishie A, Tajima T, Asayama Y, Ishigami K, Kakihara D, Nakayama T, *et al*. Diagnostic performance of apparent diffusion coefficient for predicting histological grade of hepatocellular carcinoma. Eur J Radiol 2011;80:e29–e33. doi: 10.1016/j.ejrad.2010.06.019.
14. Nakanishi M, Chuma M, Hige S, Omatsu T, Yokoo H, Nakanishi K, *et al*. Relationship between diffusion-weighted magnetic resonance imaging and histological tumor grading of hepatocellular carcinoma. Ann Surg Oncol 2012;19:1302–1309. doi: 10.1245/s10434-011-2066-8.
15. International Consensus Group for Hepatocellular Neoplasia. Pathologic diagnosis of early hepatocellular carcinoma: a report of the international consensus group for hepatocellular neoplasia. Hepatology 2009;49:658–664. doi: 10.1002/hep.22709.
16. Martins-Filho SN, Paiva C, Azevedo RS, Alves VAF. Histological grading of hepatocellular carcinoma — a systematic review of literature. Front Med (Lausanne) 2017;4:193. doi: 10.3389/fmed.2017.00193.
17. Zhou J, Lal B, Wilson DA, Laterra J, van Zijl PC. Amide proton transfer (APT) contrast for imaging of brain tumors. Magn Reson Med 2003;50:1120–1126. doi: 10.1002/mrm.10651.
18. Wang F, Numata K, Nakano M, Tanabe M, Chuma M, Nihonmatsu H, *et al*. Diagnostic value of imaging methods in the histological four grading of hepatocellular carcinoma. Diagnositics (Basel) 2020;10:321. doi: 10.3390/diagnostics10050321.
19. Pandharipande PV, Krinsky GA, Rusinek H, Lee VS. Perfusion imaging of the liver: current challenges and future goals. Radiology 2005;234:661–673. doi: 10.1148/radiol.2343031362.
20. Miles KA, Hayball M, Dixon AK. Colour perfusion imaging: a new application of computed tomography. Lancet 1991;337:643–645. doi: 10.1016/0140-6736(91)92455-b.
21. Miles KA, Charnsangavej C, Lee FT, Fishman EK, Horton K, Lee TY. Application of CT in the investigation of angiogenesis in oncology. Acad Radiol 2000;7:840–850. doi: 10.1016/s1076-6332(00)80632-7.
22. Ippolito D, Sironi S, Pozzi M, Antolini L, Invernizzi F, Ratti L, *et al*. Perfusion CT in cirrhotic patients with early stage hepatocellular carcinoma: assessment of tumor-related vascularization. Eur J Radiol 2010;73:148–152. doi: 10.1016/j.ejrad.2008.10.014.
23. Petralia G, Fazio N, Bonello L, D'Andrea G, Radice D, Bellomi M. Perfusion computed tomography in patients with hepatocellular carcinoma treated with thalidomide: initial experience. J Comput Assist Tomogr 2011;35:195–201. doi: 10.1097/RCT.0b013e31820ccf51.
24. Blomley MJ, Coulden R, Dawson P, Kormano M, Donlan P, Bufkin C, *et al*. Liver perfusion studied with ultrafast CT. J Comput Assist Tomogr 1995;19:424–433. doi: 10.1097/00004728-199505000-00016.
25. Tajima T, Honda H, Taguchi K, Asayama Y, Kuroiwa T, Yoshimitsu K, *et al*. Sequential hemodynamic change in hepatocellular carcinoma and dysplastic nodules: CT angiography and pathologic correlation. AJR Am J Roentgenol 2002;178:885–897. doi: 10.2214/ajr.178.4.1780885.
26. Patankar TF, Haroon HA, Mills SJ, Balériaux D, Buckley DL, Parker GJM, *et al*. Is volume transfer coefficient (K(trans)) related to histologic grade in human gliomas? AJNR Am J Neuroradiol 2005;26:2455–2465.
27. Edmondson HA, Steiner PE. Primary carcinoma of the liver: a study of 100 cases among 48,900 necropsies. Cancer 1954;7:462–503. doi: 10.1002/1097-0142(195405)7:3<462::aid-cncr2820070308>3.0.co;2-e.
28. Boas FE, Kamaya A, Do B, Desser TS, Beaulieu CF, Vasanawala SS, *et al*. Classification of hypervascular liver lesions based on hepatic artery and portal vein blood supply coefficients calculated from triphasic CT scans. J Digit Imaging 2015;28:213–223. doi: 10.1007/s10278-014-9725-9.
29. Kim KW, Lee JM, Klotz E, Park HS, Lee DH, Kim JY, *et al*. Quantitative CT color mapping of the arterial enhancement fraction of the liver to detect hepatocellular carcinoma. Radiology 2009;250:425–434. doi: 10.1148/radiol.2501072196.
30. Reiner CS, Gordic S, Puippe G, Morsbach F, Wurnig M, Schaefer N, *et al*. Histogram analysis of CT perfusion of hepatocellular carcinoma for predicting response to transarterial radioembolization: value of tumor heterogeneity assessment. Cardiovasc Intervent Radiol 2016;39:400–408. doi: 10.1007/s00270-015-1185-1.
31. Lee DH, Lee JM, Klotz E, Han JK. Multiphasic dynamic computed tomography evaluation of liver tissue perfusion characteristics using the dual maximum slope model in patients with cirrhosis and hepatocellular carcinoma. Invest Radiol 2016;51:430–434. doi: 10.1097/RLI.0000000000000247.
32. Heo SH, Jeong YY, Shin SS, Kim JW, Lim HS, Lee JH, *et al*. Apparent diffusion coefficient value of diffusion-weighted imaging for hepatocellular carcinoma: correlation with the histologic differentiation and the expression of vascular endothelial growth factor. Korean J Radiol 2010;11:295–303. doi: 10.3348/kjr.2010.11.3.295.
33. Van Beers BE, Leconte I, Materne R, Smith AM, Jamart J, Horsmans Y. Hepatic perfusion parameters in chronic liver disease: dynamic CT measurements correlated with disease severity. AJR Am J Roentgenol 2001;176:667–673. doi: 10.2214/ajr.176.3.1760667.
34. Sahani DV, Holalkere NS, Mueller PR, Zhu AX. Advanced hepatocellular carcinoma: CT perfusion of liver and tumor tissue — initial experience. Radiology 2007;243:736–743. doi: 10.1148/radiol.2433052020.
35. Hsu CY, Shen YC, Yu CW, Hsu C, Hu FC, Hsu CH, *et al*. Dynamic contrast-enhanced magnetic resonance imaging biomarkers predict survival and response in hepatocellular carcinoma patients treated with sorafenib and metronomic tegafur/uracil. J Hepatol 2011;55:858–865. doi: 10.1016/j.jhep.2011.01.032.
36. Asayama Y, Yoshimitsu K, Nishihara Y, Irie H, Aishima S, Taketomi A, *et al*. Arterial blood supply of hepatocellular carcinoma and histologic grading: radiologic-pathologic correlation. AJR Am J Roentgenol 2008;190:W28–W34. doi: 10.2214/AJR.07.2117.
37. Wu D, Tan M, Zhou M, Sun H, Ji Y, Chen L, *et al*. Liver computed tomographic perfusion in the assessment of microvascular invasion in patients with small hepatocellular carcinoma. Invest Radiol 2015;50:188–194. doi: 10.1097/RLI.0000000000000098.
38. Reiner CS, Goetti R, Eberli D, Klotz E, Boss A, Pfammatter T, *et al*. CT perfusion of renal cell carcinoma: impact of volume coverage on quantitative analysis. Invest Radiol 2012;47:33–40. doi: 10.1097/RLI.0b013e31822598c3.

How to cite this article: Shao CC, Zhao F, Yu YF, Zhu LL, Pang GD. Value of perfusion parameters and histogram analysis of triphasic computed tomography in pre-operative prediction of histological grade of hepatocellular carcinoma. Chin Med J 2021;134:1181–1190. doi: 10.1097/CM9.0000000000001446